

Multidisciplinary wing design and optimization for transport aircraft

Tobias F. Wunderlich

DLR Institute of Aerodynamics and Flow Technology

Lilienthalplatz 7, 38108 Braunschweig, Germany

tobias.wunderlich@dlr.de

Telephone +49 531 295-2816

Telefax +49 531 295-2320

September 22, 2008

Abstract

The design of a transonic wing is a multidisciplinary task. The aim is to consider all the interactions of the relevant disciplines in wing design in one optimization process. Only high fidelity methods are able to model the physics in this flight regime accurately. In this work, an optimization of a transonic wing for cruise conditions with CFD for the aerodynamics and FEM for the structure is presented. This includes the development of an optimization chain with a fluid-structure coupling procedure. A feasible sizing algorithm, a meaningful objective function and an optimization strategy to find the global optimum are considered as well. First results for wing planform optimization and wing shape optimization based on coupled fluid-structure simulations are presented. Finally, the paper discusses the planned future developments of the described optimization chain.

Keywords

Multidisciplinary Optimization (MDO), Fluid-Structure Coupling, Transonic Wing Optimization

1 Introduction

Future transport aircraft development is driven by more stringent regulations and the need to improve efficiency, performance and passenger comfort. Two options have to be considered. The first one is to find new aircraft concepts and the other one is the further development of the conventional aircraft configuration. The combination of increasing computer resources and advanced numerical simulation tools

allow for an accurate prediction of flight performance of an aircraft configuration. This includes the fluid-structure coupling of the aircraft wing for a given structure model with high fidelity methods [14]. On the one hand, the consideration of the interaction of the disciplines in aircraft design is essential. On the other hand, the physics have to be represented with accurate simulation tools. High fidelity tools need a detailed description of the geometry. An appropriate parametrization of the surface and structure geometry is a fundamental precondition for finding new concepts.

Numerical optimization is one approach for the design and improvement of aircraft configurations. This paper describes a process chain and its components for the numerical optimization of a conventional transonic aircraft configuration. A flight mission was selected to include the aerodynamic performance and the structure weight in the objective function of the multidisciplinary optimization. At a single point of the cruise flight, the aerodynamic performance has been calculated with a fluid-structure coupled procedure. It is difficult to consider all the relevant load cases. In this work, only load cases derived from the cruise flight loads are included. Thereby, the integration of the wing box sizing in the coupling process is suitable.

The flight range for a given aircraft configuration was estimated for the selected parameter settings. Parameters of the wing, like the sweep angle, twist angles, aspect ratio, taper ratio and airfoil thicknesses, affect the transonic aerodynamic performance and the load distribution of the elastic wing. The aerodynamic loads impact the wing weight of the iterative deformed wing by the integrated wing box sizing algorithm. Airfoil form parameters primarily affect the aerodynamic coefficients. Aerodynamic twist modifications change the lift distribution in spanwise direction and thereby the wing weight.

2 The Process Chain and its Components

The process chain consist of running in sequence programs. To account for the deformation of the wing due to the aerodynamic loads and the sizing of the structure, a complex program chain was needed. All programs in the process chain have to run automatically without user interfaces. The optimization chain consists of:

- Parametric CAD model updating,
- Aerodynamic grid generation or deformation,
- Structural grid generation,
- CFD analysis,
- FEM analysis and structure sizing,
- Interpolation sequences for fluid-structure coupling,
- Aerodynamic mesh deformation.

In Fig. 1, the program chain is illustrated. The fluid-structure coupling loop stops when the tip deflection, twist angle, lift over drag ratio, wing mass, fuel mass and

the flight range are converged. Thereby, the coupling loop includes the structural sizing of the wing box. The result of the process chain is a sized wing in the static aeroelastic equilibrium. Furthermore, aerodynamic performance, structure weight and flight range are known for this investigated wing.

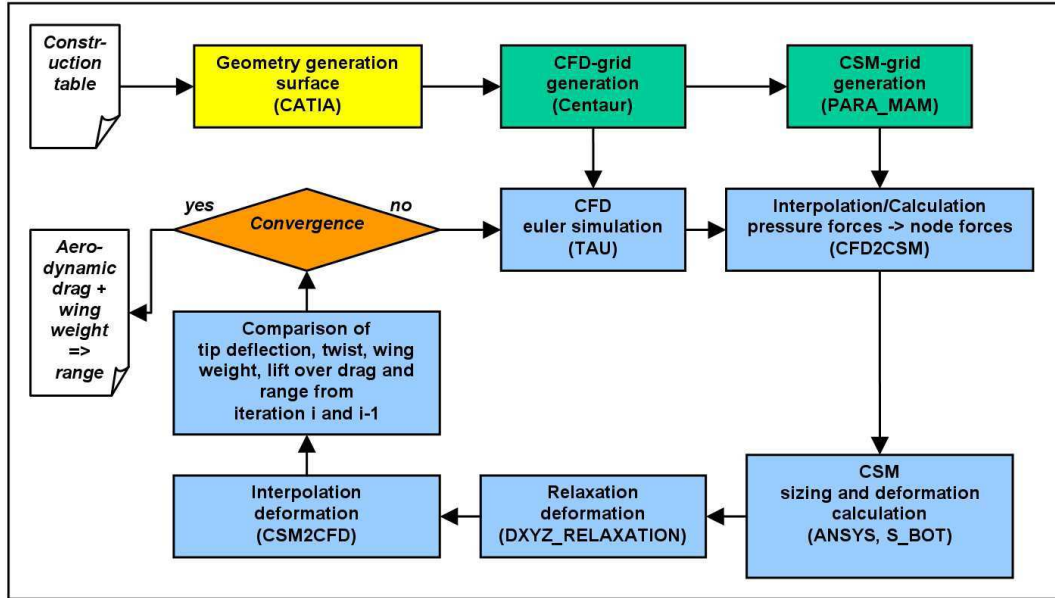


Figure 1: Process chain

2.1 Flight Mission

A simple model for the flight mission was selected. This model is described in [1] and often used for preliminary aircraft design. In this work, the flight mission consist of five segments. The objective function for this multidisciplinary wing

Segment No.	Mission segment	Weight fraction	Reference
1	Warmup and take-off	$(W_1/W_0) = 0.980$	[1]
2	Climb and accelerate	$(W_2/W_1) = 1.0065 - 0.0325Ma_{cruise}$	[1]
3	Cruise	$(W_3/W_2) = \text{calculated with process chain}$	
4	Descent for landing	$(W_4/W_3) = 0.993$	[1]
5	Landing and taxi	$(W_5/W_4) = 0.995$	[1]

Table 1: Flight mission segment weight fractions

optimization is the range. A generic long range transport aircraft configuration was selected for all described investigations. The selected maximum take-off mass m_{MTO} and payload $m_{payload}$ is given in Table 2.1. With a selected value of 0.2, the payload to maximum take-off mass ratio is a typical value for long range transport aircrafts. Assumptions were made for the wing structure mass to wing mass ratio $m_{wing\ structure}/m_{wing}$ and the structure mass ratio of the whole aircraft without the wing $m_{structure\ w/o\ wing}/m_0$. The values are also given in Table 2.1. The wing

loading for the maximum take-off mass m_0 was set to $m_0/S = 625 \text{ kg/m}^2$. This selection guarantees good take-off and landing performance with a typical high lift system. Thereby, the wing area results in a value of $S = 360 \text{ m}^2$ for this aircraft. For the cruise segment of the flight mission a Mach number of $Ma = 0.85$ and a

Maximum take-off mass	m_0	225000 kg
Payload	$m_{payload}$	45000 kg
Wing structure mass to wing mass ratio	$m_{wing \text{ structure}}/m_{wing}$	0.6
Structure mass without the wing to maximum take-off weight ratio	$m_{structure \text{ w/o wing}}/m_0$	0.329
Reserve fuel mass to fuel mass ratio	$m_{reserve \text{ fuel}}/m_{fuel}$	0.06
Wing loading	m_0/S	625 kg/m^2
Wing area	S	360 m^2

Table 2: Masses and weight fractions of the selected aircraft configuration

flight altitude of 35000 ft ($FL = 350$) was selected. Furthermore, a 6% reserve and trapped fuel ratio $m_{reserve \text{ fuel}}/m_{fuel}$ is assumed.

The fluid structure coupling procedure calculates the lift to drag ratio and the mass of the sized wing structure for the aerostatic equilibrium. All process steps are described in detail in the next sections. The aerodynamic drag coefficient consists of a constant value of $C_{D, \text{ fuselage/tailplane/engine}} = 0.012$ for the fuselage, tailplanes and engines, the pressure drag coefficient of the wing $C_{Dp, \text{ wing}}$ and the viscous drag coefficient of the wing $C_{Dv, \text{ wing}}$. With the value of the wing structure mass, the fuel mass can be estimated. The total fuel tank volume is checked for the required volume of the fuel. If there is not enough space for the fuel in the wing box, the fuel mass for maximal filled fuel tanks will be used. The mission weight fraction will be calculated with (1) and all selected masses and weight fractions are given in Table 2.1.

$$\frac{W_5}{W_0} = 1 - \frac{1 - (m_{payload}/m_0) - (m_{structure \text{ w/o wing}}/m_0) - (m_{wing}/m_0)}{1 + (m_{reserve \text{ fuel}}/m_{fuel})} \quad (1)$$

The mission weight fractions of Table 2.1 deliver the cruise weight fraction (2).

$$\frac{W_3}{W_2} = \frac{(W_5/W_0)}{(W_1/W_0) (W_2/W_1) (W_4/W_3) (W_5/W_4)} \quad (2)$$

Hence, the range will be calculated with the Breguet range equation (3). This implies an increasing fuel mass ratio for a decrease in wing structure mass. The specific fuel consumption (SFC) in the range equation (3) is set to 0.5 kg/kg h for high-bypass turbofan engines under cruise flight conditions [1].

$$R = \frac{V}{SFC} \frac{L}{D} \ln \frac{W_3}{W_2} \quad (3)$$

2.2 Parametric CAD Model

The parametric CAD model was built in CATIA V5 [5]. To change the geometry, a construction table is linked to the model. The trapezoid wing geometry is

constructed with an inner and an outer airfoil section. Parameters for the wing planform are the aspect ratio Λ , the leading edge sweep angle φ , the taper ratio λ , the twist angle ε and the dihedral angle ν . The airfoils are parameterized with the Class function/Shape function Transformation technique (CST) [2], [3]. The airfoil thickness is an additional parameter to scale the thickness to chord ratio in each airfoil section. For the parametrization of the airfoil geometry, an additional tool is used [4]. At first, this tool calculates the Bernstein polynomial coefficients of a given airfoil geometry. A table of the Bernstein polynomial coefficients is linked with the optimization framework. To get the modified airfoil shape, the parametrization tool calculates the geometry of the airfoil from a new set of Bernstein polynomial coefficients. A CATIA makro reads the points of the changed airfoil geometry and replaces the airfoil shape in the CATIA wing model. The viscous drag coefficient of the wing $C_{Dv, wing}$ is estimated. For this a flat plate analogy integrated over the trapezoid wing for turbulent flow (4), (5) is used. The Reynolds numbers $Re_{section 1}$ and $Re_{section 2}$ are calculated for the cruise flight condition.

$$C_{Dv, wing} = \frac{37}{225} \frac{Re_{section 1}^{4/5} - \lambda Re_{section 2}^{4/5}}{Re_{section 1} (1 + \lambda) (1 - \lambda)} FF \quad (4)$$

$$FF = 1 + 2 \left(\frac{t}{c} \right) + 100 \left(\frac{t}{c} \right)^4 \quad (5)$$

2.3 Aerodynamic Grid Generation Process

For grid generation, the software Centaur [6] is used. The unstructured grid generation process is adequate for all geometric model variations. When only the airfoils of the wing are modified, a grid deformation tool replaces the complete grid generation. Fig. 2 shows the unstructured surface grid of the trapezoid wing. The surface is meshed with triangles and the volume mesh consists of tetrahedrons. The unstructured grid of the wing consists of approximately 500000 grid points.

2.4 Flow solver

The transonic flow around the wing is simulated with the DLR TAU-Code [8], [9], [10], which is developed at the DLR Institute of Aerodynamics and Flow Technology. The TAU-Code solves the compressible, three-dimensional Reynolds-Averaged Navier-Stokes equations. The TAU code is a well established tool for aerodynamic applications at DLR, universities and aerospace industry [11], [12], [13]. The TAU code uses a vertex centered dual mesh formulation. For spatial approximation, a finite-volume method with second order upwind or central discretization is used. Only for testing the optimization chain, the viscous terms have not been considered.

2.5 Structural Grid Generation Process

Structural models of the wing are obtained using the DLR wing generation tool PARA_MAM (Parametric, Simple and Fast Mesh Based Aircraft Modelling Tool)

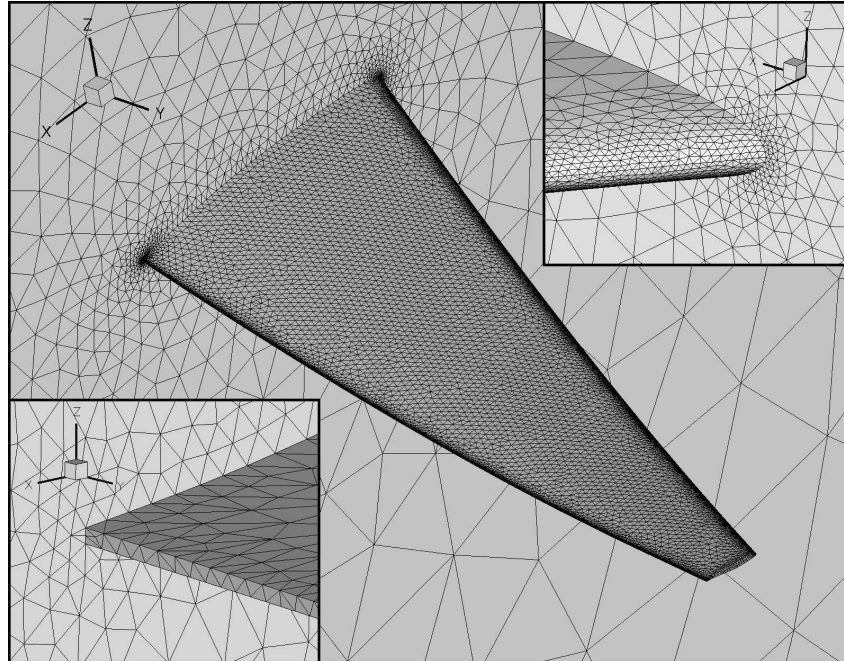


Figure 2: Unstructured surface grid of a trapezoid wing. Enlargements show trailing edge and leading edge regions.

[7], which is developed at the DLR Institute of Composite Structures and Adaptive Structures. Based on a full parametric description of the inner structure and the aerodynamic surface mesh, all geometric keypoints are calculated and subsequently output as complete input deck for the finite element analysis pre-processor. The structure model of the wing consists of realistically arranged spars and ribs and a multi-layered skin. The stringers are modeled as "smeared" stiffness of the skin.

Fig. 3 shows the inner structure of a wing. In this case, the wing box structure consists of a front spar at 0.15 chord length, a rear spar at 0.70 chord length and 39 ribs parallel to the flight path.

2.6 Structural Analysis and Sizing

The finite element analysis software for the structure evaluation is ANSYS [17]. The sizing is performed with the program S_BOT (Sizing Robot). This tool is a suite of macros written at DLR Institute of Composite Structures and Adaptive Structures in the ANSYS Parametric Design Language (APDL). S_BOT is an infrastructure to automatically analyse multiple load cases. The input for S_BOT are an FEM model and sets of external aerodynamic loads. The definition of all load cases includes:

- Aerodynamic loads,
- Gravity acceleration,
- Engine forces,
- Tank weight forces,

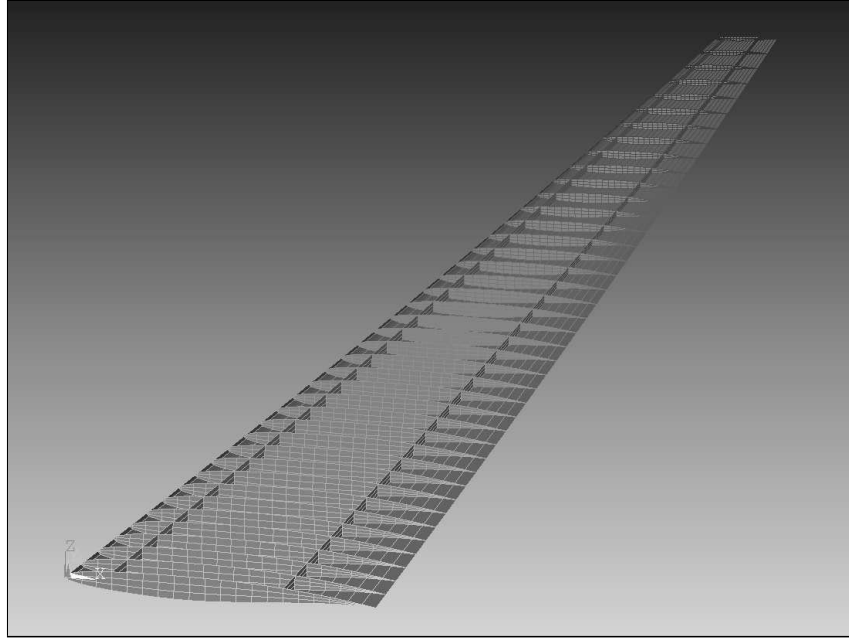


Figure 3: Inner structure of a trapezoid wing

- Gear forces,
- Definition of structural limits (yield strength, fatigue strength).

The forces remain constant during the sizing loop. Only in PARA_MAM defined optimization regions of the wing structure are taken into account for the sizing algorithm. The abort criterium of the sizing loop is a user specified value for convergence of the wing structure mass. In this work three load cases were selected for the structural sizing of the wing. The load cases are shown in table 2.6.

Load case	Aerodynamic loads	Gravity acceleration	Structural limit
Cruise flight	Cruise flight loads	1.0 <i>g</i>	fatigue strength
2.5 <i>g</i> maneuver	Cruise flight loads scaled with 2.5	2.5 <i>g</i>	yield strength
Touch-down	-	1.3 <i>g</i>	yield strength

Table 3: Selected load cases for the structural sizing of the wing

2.7 Interpolation Module

An interpolation tool MESH2MESH [14] interpolates the aerodynamic surface pressure distribution to the nodal forces for the structure mesh. This interpolation tool is developed at DLR Institute of Aerodynamics and Flow Technology. After the evaluation of the structure deformation, the tool MESH2MESH interpolates the nodal displacements of the structure mesh to the aerodynamic surface grid. For the mapping of aerodynamic loads from the CFD to the CSM coupling surface the nearest neighbor search for the pressure coefficient is selected. In contrast to using the linear interpolation, this selection ensures a conservative interpolation scheme with

respect to forces and moments. The volume-spline interpolation [15] is used for the mapping of deflections from the CSM coupling surface back to the CFD coupling surface. This technique is appropriate for smooth functions like the deformation of aircraft wings.

2.8 Aerodynamic Mesh Deformation

The deformation module of the TAU-Code deforms the aerodynamic grid for the aero-structure coupling procedure. The interpolation tool MESH2MESH calculates the deformed surface grid. The deformation tool of the TAU-Code determines the volume grid with the original surface grid and the deformed surface grid. The developed algebraic method [16] for the grid deformation module of the TAU-Code is robust for small displacements [14].

3 Transonic Wing Optimization

3.1 Planform Optimization

A first fluid-structure coupled wing planform optimization was performed. The parameters for this optimization were sweep angle, aspect ratio, thickness and twist angle of the wing. The objective function for this optimization was the range. For a robust and efficient search of the global optimum the Subplex algorithm [18] is used. The optimization history for range, lift over drag ratio and wing mass is shown in Fig. 4. The optimization converged within 110 function evaluations. For each function evaluation 6 – 10 coupling iterations are performed to reach the static aeroelastic equilibrium. For some parameter settings, the process chain was not able to find a solution. The range for these configurations was set to 10% of the former value. The attempt to make the process more robust results in a modified aerodynamic solver setting. For this reason, the maximum of the range of iteration 38 was not reached again, but the geometry of the optimized wing is nearly the same. The variation of the geometric parameters over the optimization process is shown in Fig. 5. To reduce the transonic wave drag, the sweep angle has been increased and the airfoil thickness of the root section of the wing has been decreased. The aspect ratio has been decreased to reduce the structural mass of the wing and to carry more fuel in the wing. The optimization history of the wing mass and the fuel mass are shown in Fig. 6. In Fig. 7, the tip deflection difference between the rigid and the elastic wing is presented. A wing tip deflection of 2 m for the optimized wing indicates a highly flexible wing design. Only a multipoint wing design can answer the question of wing stiffness in respect to aerodynamic performance. Furthermore, the twist angle difference shows the bending and torsion coupling of the backward swept wing.

The induced drag C_{Di} of planar wings is minimal for the elliptical lift distribution. The circulation distributions for the initial and the optimized wing are shown in Fig. 8. The circulation distribution is plotted over the dimensionless spanwise coordinate η . The increased aspect ratio of the optimized wing results in a lower wing span for the same wing area. So the level of the local circulation γ at the same dimensionless spanwise position is greater for the optimized wing than for the initial wing. To unload the wing tips and to reduce the structural mass of the

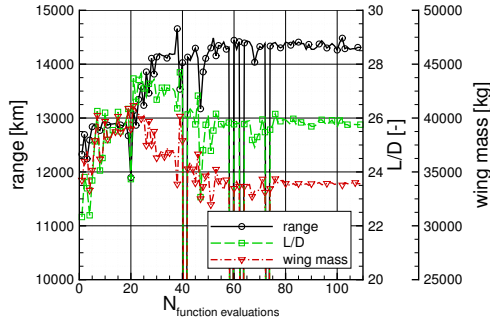


Figure 4: Optimization history of flight range, lift over drag ratio and wing mass

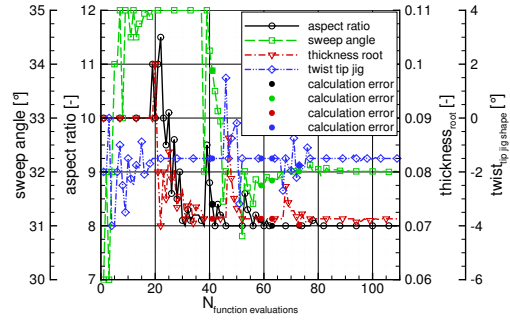


Figure 5: Optimization history of sweep angle, aspect ratio, thickness and twist angle

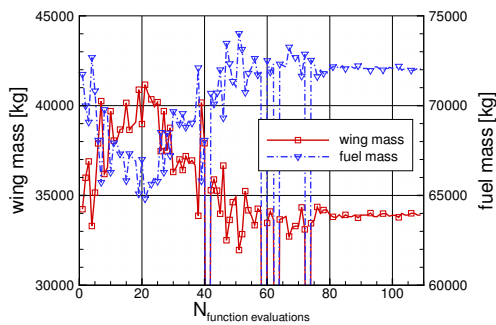


Figure 6: Optimization history of wing mass and fuel mass

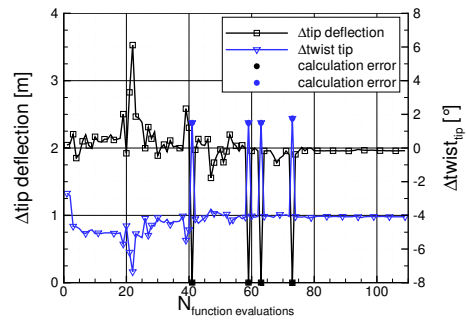


Figure 7: Optimization history of tip deflection difference and twist angle difference

wing, the circulation has to increase inboards and decrease outboards. Both of the investigated wings have a similar circulation distribution which saves weight but comes with a drag penalty. The circulation distribution of the optimized wing is a little closer to the elliptical distribution. The local lift coefficient of the optimized wing is higher in the outboard region and lower near the wing root. The maximum local lift coefficient of the optimized wing is smaller than the maximum value of the initial wing. The deflection z and the twist angle ε for the initial and the optimized wing are shown in Fig. 9 versus the spanwise coordinate η . In the Fig. 10, the Mach number distribution on the wing surface is plotted for the initial and the optimized wing. To compare the wings, Fig. 11 to Fig. 14 additionally show the Mach number in four airfoil sections. On the upper side of the wing, the transonic shock near the trailing edge is reduced during the planform optimization. A weaker second shock appears in the front of the airfoils. The reduction of the wing root airfoil thickness ratio results in a lower Mach number on the upper side of the wing.

To evaluate the performed fluid-structure coupled wing optimization, the polars of the initial and optimized wing are computed (Fig. 15). These polars include the deformation of the sized wings. For comparison, the rigid polars are calculated additionally. The aerodynamic performance of the optimized wing is better as the

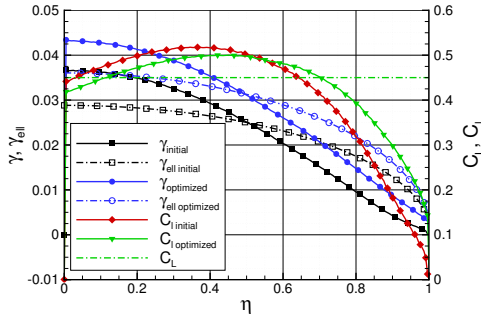


Figure 8: Circulation distribution and local lift coefficient of the initial and the optimized wing

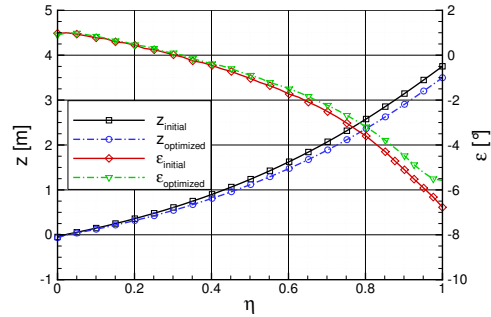


Figure 9: Local deflections and twist distribution of the initial and the optimized wing

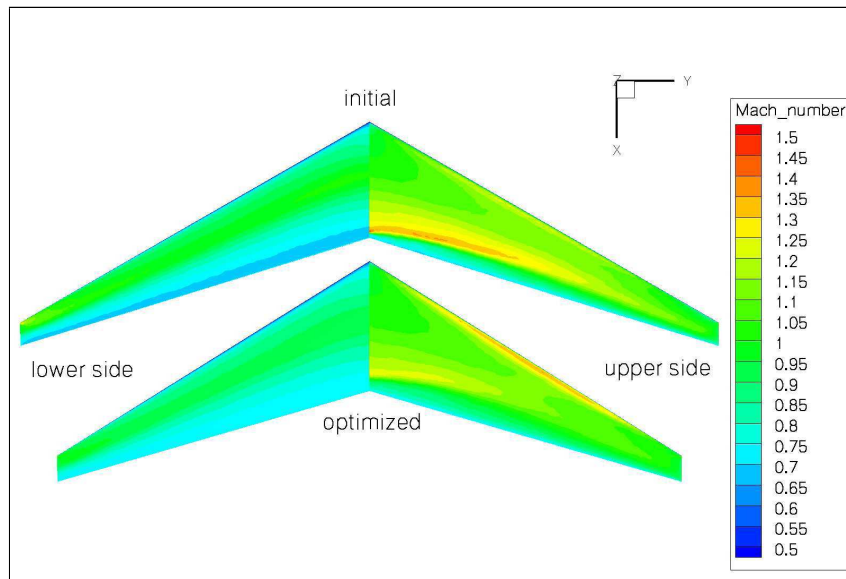


Figure 10: Mach distribution of the initial and the optimized wing

initial wing over the range of investigated lift coefficients.

3.2 Airfoil Optimization

Without modifying the airfoil shape, the wing optimization is limited. To investigate the influence of the airfoil shape variation another fluid-structure optimization is performed. The parameters for this optimization changed the upper side of the wing. The initial airfoil geometry in the inner and outer section of the wing was the RAE2822 airfoil. The airfoil was scaled to a thickness to chord ratio of $t/c = 0.09$. The upper side of the airfoil was parametrized with five Bernstein polynomial coefficients of the CST-method. The geometry parameters for this optimization were these five polynomial coefficients. The objective function for this optimization was also the range. The optimization history for range, lift over drag ratio and wing mass is shown in Fig. 16. The optimization was converged after 34 function evaluations. For some parameter settings, the process chain was not able to find a solution.

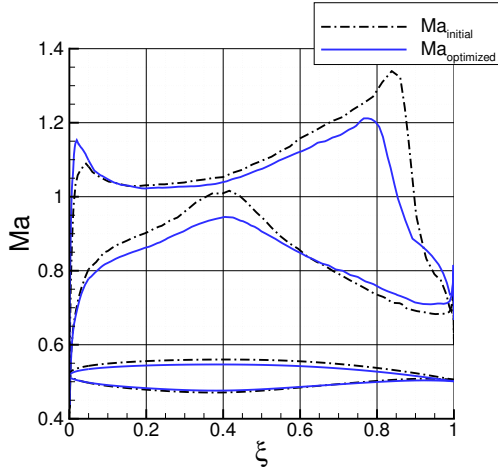


Figure 11: Mach distribution at $\eta = 0.10$

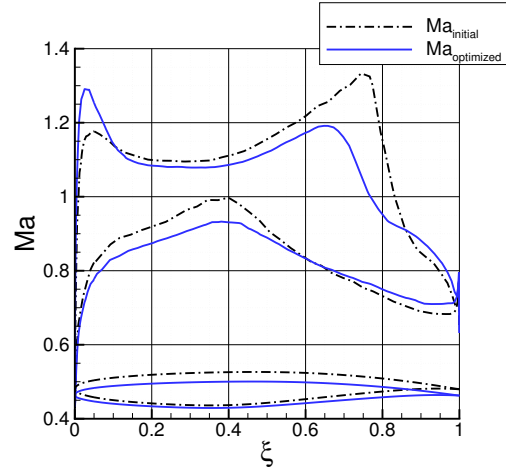


Figure 12: Mach distribution at $\eta = 0.30$

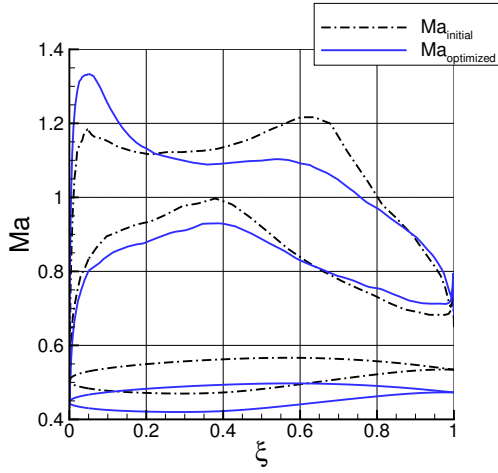


Figure 13: Mach distribution at $\eta = 0.60$

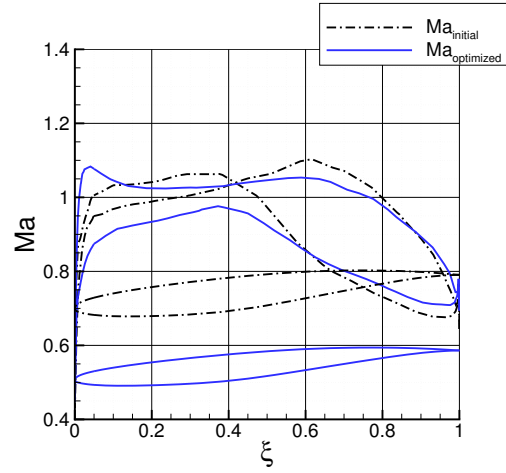


Figure 14: Mach distribution at $\eta = 0.90$

In Fig. 17 the Mach distribution of the initial and the optimized wing surface are shown. In Fig. 18 to Fig. 21 the Mach number distributions in four airfoil sections are plotted. The transonic shock is reduced over the wing and the drag coefficient is decreased. The aerodynamic performance is increased and the wing structure mass is nearly unchanged. The airfoil shape optimization shows a strong impact on the transonic flight performance. Hence, the airfoil shape modification has to be considered in the transonic multidisciplinary wing design and optimization. The problem is to reduce the number of airfoil parameters to an applicable quantity for this time-consuming fluid-structure optimization.

4 Conclusion and Future Work

The discussed fluid-structure process chain is adequate for multidisciplinary wing planform and airfoil shape optimizations with a small number of parameters. Some

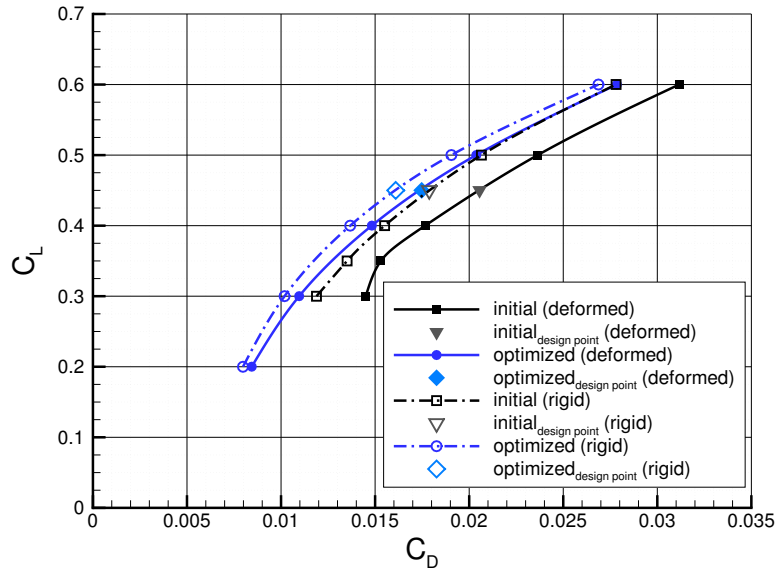


Figure 15: Polars of the initial and the optimized wing

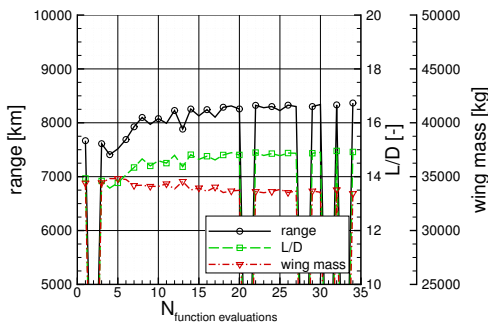


Figure 16: Optimization history of flight range, lift over drag ratio and wing mass

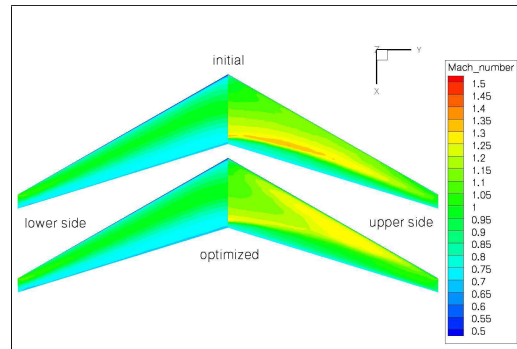


Figure 17: Mach distribution of the initial and the optimized wing

problems with the robustness of the process chain have to be solved. The computation time for the process chain has to be reduced.

The number of load cases has to be extended. The $2.5 g$ maneuver load case is the most important one for the structural sizing algorithm. The aim is to calculate the loads for this load case with the fluid-structure coupled process chain. For the cruise flight only the aerodynamic performance and the loads in the aerostatic equilibrium are relevant. A future approach is to analyse the flight shape for the aerodynamic performance and the loads in the cruise flight. This shape is used for the calculation of the fluid-structure coupled wing deformation in the $2.5 g$ maneuver. This new approach creates realistic loads for the critical maneuver load case. A multipoint optimization has to be performed in order to analyse the influence of the wing stiffness of the flexible wing on the flight performance. Furthermore, a double trapezoid wing planform will be used for a future fluid-structure coupled wing optimization.

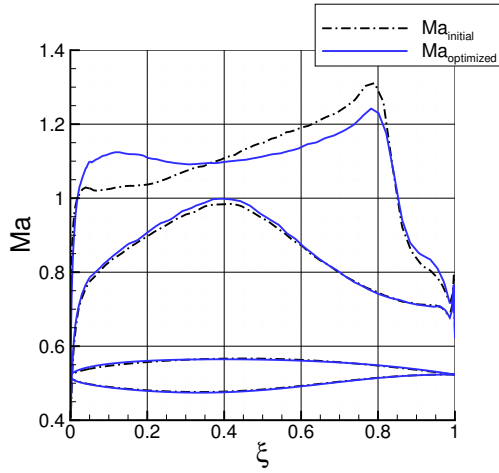


Figure 18: Mach distribution at $\eta = 0.10$

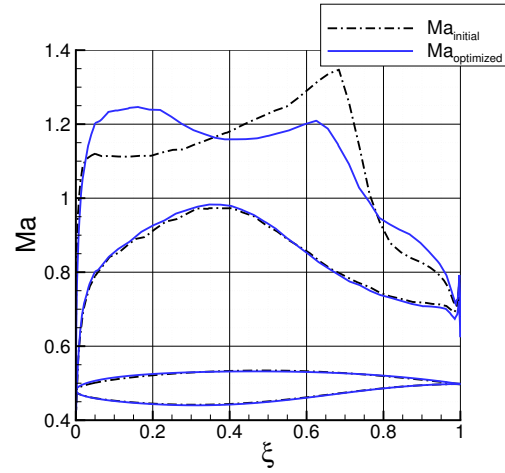


Figure 19: Mach distribution at $\eta = 0.30$

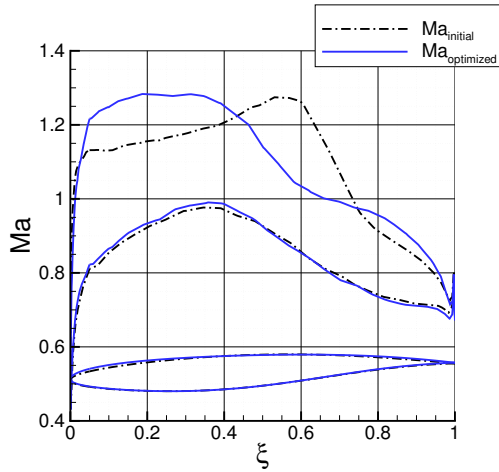


Figure 20: Mach distribution at $\eta = 0.60$

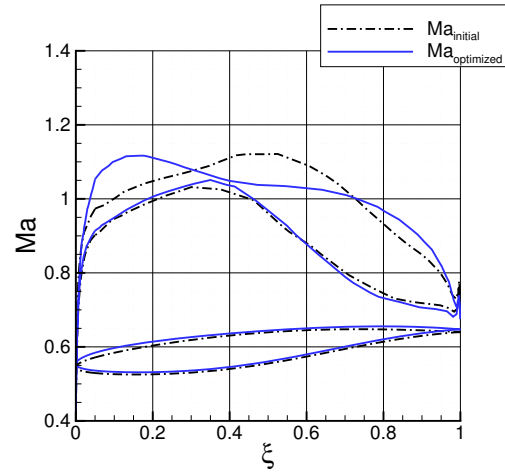


Figure 21: Mach distribution at $\eta = 0.90$

5 Acknowledgement

The author wish to thank the Institute of Aerodynamics and Flow Technology at the German Aerospace Center for providing the support of many colleagues and the computational resources for the complex computations.

References

- [1] Raymer, D.P.: "Aircraft Design: A Conceptual Approach", Third Edition, American Institute of Aeronautics and Astronautics, Inc., Reston, Virginia, 1999.

- [2] Kulfan, B.M.; Bussoletti J.E.: "Fundamental Parametric Geometry Representations for Aircraft Component Shapes", Boeing Commercial Airplane Group, AIAA 2006-6948, 2006.
- [3] Kulfan, B.M.: "A Universal Parametric Geometry Representation Method-"CST"", Boeing Commercial Airplane Group, AIAA 2007-62, 2007.
- [4] Sattler, S.: "Vergleich und Bewertung von Parametrisierungsmethoden zur Optimierung von transsonischen Tragflügelprofilen", Diploma Thesis TU Braunschweig, 2008.
- [5] <http://www.catia.com>
- [6] <http://www.centaursoft.com>
- [7] Nagel, B.; Rose, M.; Monner, H.P.; Heinrich, R.: An Alternative Procedure for FE-Wing Modelling, DGLR-2006-048, DGLR Annual Conference, Braunschweig, Germany, 2006.
- [8] Galle, M.: Ein Verfahren zur numerischen Simulation kompressibler, reibungsbehafteter Strömungen auf hybriden Netzen, DLR-FB 99-04, 1999.
- [9] Gerhold, Th.: Overview of the Hybrid RANS TAU-Code, In: Kroll, N., Fassbender, J. (Eds) MEGAFLOW Numerical Flow Simulation Tool for Transport Aircraft Design, Notes on Multidisciplinary Design, Vol. 89, Springer, 2005.
- [10] Schwamborn, D.; Gerhold, T.; Heinrich, R.: The DLR TAU-Code: Recent Applications in Research and Industry, In proceedings of European Conference on Computational Fluid Dynamics ECCOMAS CDF 2006, Delft, The Netherlands, 2006.
- [11] Kroll, N.; Fassbender, J. K. [Hrsg.]: MEGAFLOW - Numerical Flow Simulation for Aircraft Design, Notes on Numerical Fluid Mechanics and Multidisciplinary Design (NNFM), 89, Springer, Closing Presentation DLR Project MEGAFLOW, Braunschweig, Germany, ISBN 3-540-24383-6, 2002.
- [12] Kroll, N., Rossow, C.C., Schwamborn, D., Becker, K., Heller, G.: MEGAFLOW - A Numerical Flow Simulation Tool For Transport Aircraft Design, ICAS Congress 2002, Toronto, Canada, ICAS-Proceedings, pp 1.105.1-1.105.20, 2002.
- [13] Kroll, N., Rossow, C.C., Schwamborn, D.: The MEGAFLOW-Project - Numerical Flow Simulation for Aircraft. In A. DiBucchianico, R.M.M. Mattheij, M.A. Peletier (Edts.), Progress in Industrial Mathematics at ECMI 2004, Springer, New York, S. 3 33, 2005.
- [14] Kroll, N.; Heinrich, R.; Krueger, W.; Nagel, B.: Fluid-Structure Coupling for Aerodynamic Analysis and Design: A DLR Perspective, AIAA 2008-561, 46th AIAA Aerospace Sciences Meeting and Exhibit, Reno, Nevada, 2008.

- [15] Beckert, A., Wendland, H.: Multivariate interpolation for fluid-structure-interaction problems using radial basis functions, *Aerospace, Science and Technology* 5 (AST), pp 125-134, 2001.
- [16] Gerhold, T.: Efficient Algorithms for Mesh, Deformation, Proceedings of the ODAS Symposium Toulouse, 2006.
- [17] <http://www.ansys.com>
- [18] Wild, J.: Numerische Optimierung von zweidimensionalen Hochauftriebskonfigurationen durch Lösung der Navier-Stokes-Gleichungen, Dissertation TU Braunschweig, DLR-FB 2001-11, 2001.